Neutral high-generation phosphorus dendrimers inhibit macrophage-mediated inflammatory response in vitro and in vivo

I. Posadas[a,b,c], L. Romero-Castillo[a,b], N. El Brahmi[d,e,f], D. Manzanares[a,b], S. Mignani[g,h], J.-P. Majoral[d,e,f], and V. Ceña[a,b,1]

[a]Unidad Asociada Neurodeath, Universidad de Castilla-La Mancha, 02006 Albacete, Spain; [b]Centro de Investigación Biomédica en Red para Enfermedades Neurodegenerativas, 28031 Madrid, Spain; [c]Facultad de Farmacia, Universidad de Castilla-La Mancha, Albacete, Spain; [d]Laboratoire de Chimie de Coordination, CNRS, BP 44099, F-31077, France; [e]Université de Toulouse, Université Paul Sabatier, Institut National Polytechnique de Toulouse, F-31077, France; [f]Euromed Research Institute, Euro-Mediterranean University of Fes, 30000 Fes, Morocco; [g]Laboratoire de Chimie et de Biochimie Pharmacologiques et Toxicologique, Université Paris Descartes, Pôle de Recherche et d'Enseignement Supèrieur Sorbonne Paris Cité, CNRS UMR 860, 75006 Paris, France; and [h]Centro de Química da Madeira, Molecular Materials Research Group, Universidade da Madeira, 9020-105 Funchal, Portugal

Edited by Michael L. Klein, Temple University, Philadelphia, PA, and approved July 21, 2017 (received for review March 24, 2017)

Inflammation is part of the physiological response of the organism to infectious diseases caused by organisms such as bacteria, viruses, fungi, or parasites. Innate immunity, mediated by mononuclear phagocytes, including monocytes and macrophages, is a first line of defense against infectious diseases and plays a key role triggering the delayed adaptive response that ensures an efficient defense against pathogens. Monocytes and macrophages stimulation by pathogen antigens results in activation of different signaling pathways leading to the release of proinflammatory cytokines. However, inflammation can also participate in the pathogenesis of several diseases, the autoimmune diseases that represent a relevant burden for human health. Dendrimers are branched, multivalent nanoparticles with a well-defined structure that have a high potential for biomedical applications. To explore new approaches to fight against the negative aspects of inflammation, we have used neutral high-generation phosphorus dendrimers bearing 48 (G3) or 96 (G4) bisphosphonate groups on their surface. These dendrimers show no toxicity and have good solubility and chemical stability in aqueous solutions. Here, we present data indicating that neutral phosphorus dendrimers show impressive antiinflammatory activities both in vitro and in vivo. In vitro, these dendrimers reduced the secretion of proinflammatory cytokines from mice and human monocyte-derived macrophages. In addition, these molecules present efficient antiinflammatory activity in vivo in a mouse model of subchronic inflammation. Taken together, these data suggest that neutral G3-G4 phosphorus dendrimers have strong potential applications in the therapy of inflammation and, likely, of autoimmune diseases.

dendrimers | inflammation | innate immunity | air pouch | macrophage

Inflammation is a physiological response of the organism for its defense against several insults, mainly infectious diseases, and it is part of the body's immune response. However, inflammation can also participate in the pathogenesis of several diseases including central nervous system (named CNS) diseases such as multiple sclerosis, where peripheral mononuclear phagocytes infiltrate the CNS and participate in the induction and development of the disease (1, 2) or Alzheimer's disease, where β-amyloid deposits represent a key pathological effect. Mononuclear phagocytes, including monocytes and macrophages, play a central role in innate immunity as a first line of defense and also ensure the delayed adaptive immune response. Monocytes and macrophages are a heterogeneous population encompassing a large spectrum of phenotypes depending on the stimulus type (3). Monocytes and macrophages stimulation by lipopolysaccharides (LPS) results in nuclear translocation of the nuclear factor-*kappa B* (NFkB), polarization of the macrophages to the classical activation pathway (M1 population), the release of proinflammatory cytokines such as tumor necrosis factor (TNFα), interleukins 1 and 6 (IL-1, IL-6), and the expression of cyclin-dependent kinase 86 (CD86) (4).

An alternative M2 differentiation phenotype is also activated in macrophages. M2 polarization is accompanied by secretion of antiinflammatory cytokines such as IL-10, IL-4, expression of CD163, and down-regulation of proinflammatory mediators such as TNFα, IL-1β, and CD86 (5, 6). Thus, macrophages play a central role in triggering and resolving inflammation (7), and modulation of M1/M2 ratio is a promising strategy to achieve resolution of inflammation in situations where it is detrimental for the organism.

Dendrimers are branched, multivalent nanoparticles with a well-defined structure. These macromolecules are globular and nanoscaled with a particular architecture formed by three distinct domains: a central core having at least two chemical functionalities to allow branches linkage; branches composed of repeated units leading to a series of radially concentric layers named generations (G), and terminal functional groups that facilitate interactions with molecules of the environment. While polycationic dendrimers (8) and in particular polycationic phosphorus dendrimers can be used as transfecting agents and cargo for the delivery of nucleic acids or drugs into cells (9–12), some other phosphorus dendrimers capped with trimannopyranosides allow reduction of lung accumulation of neutrophils in a mouse model of acute lung inflammation (13). Some other

Significance

Inflammation is a relevant part of the physiological response of the immune system to fight infectious diseases. However, excessive inflammation can also participate in the pathogenesis of several diseases. To open new avenues to treat the negative aspects of inflammation, we have used biocompatible nanoparticles, neutrally charged G3-G4 phosphorus dendrimers, which are not toxic and have good solubility and chemical stability in aqueous solutions. These nanoparticles are very efficient, in vitro and in vivo, to tackle the inflammatory response produced by different agents. In addition, the high number of chemically modifiable terminal groups on the surface of these nanodevices opens the high possibility of incorporating into them specific therapeutic groups which provide multifunctional therapeutic abilities.

Author contributions: S.M., J.-P.M., and V.C. designed research; I.P., L.R.-C., N.E.B., and D.M. performed research; N.E.B., S.M., and J.-P.M. contributed new reagents/analytic tools; I.P., L.R.-C., D.M., J.-P.M., and V.C. analyzed data; and J.-P.M. and V.C. wrote the paper.

Conflict of interest statement: J.-P.M. filed the patent 2010WO2010013086A1 entitled: "Phosphorylated dendrimers as anti-inflammatory drugs"; the patent refers only to biphosphonic dendrimers which are polyanionic and not neutral as the G3bis and G4bis dendrimers used in this article. For this reason, we consider that there is no conflict of interest.

This article is a PNAS Direct Submission.

[1]To whom correspondence should be addressed. Email: valentin.cena@gmail.com.

This article contains supporting information online at www.pnas.org/lookup/suppl/doi:10.1073/pnas.1704858114/-/DCSupplemental.

members of the phosphorus dendrimer family, more precisely a polyanionic phosphorus dendrimer of generation 1 bearing 12 aza bisphosphonic groups on its surface, has shown antiinflammatory properties on isolated monocyte/dendritic cells (14, 15) and in a model of experimental arthritis (16).

To open new avenues to fight against diverse aspects of inflammation, it was of interest to investigate the properties of neutral phosphorus dendrimers and more particularly of dendrimers of higher generation bearing 48 (G3) or 96 (G4) bisphosphonate groups on their surface. The choice of these terminal groups was dictated by the absence of cytotoxicity of these dendrimers as well as their good solubility and chemical stability. Here, we present original studies indicating that these two phosphorus dendrimers show a significant antiinflammatory activity both in vitro by reducing the secretion of proinflammatory cytokines by tissue macrophages in mice as well as in vivo in a mouse model of subchronic inflammation, suggesting that this family of noncharged dendrimers might have potential applications in the therapy of inflammation and, likely, of autoimmune diseases.

Results

Effect of Neutral Phosphorus Dendrimers G3bis and G4bis on Mouse Peritoneal Macrophages Viability. Mouse peritoneal macrophages were treated with increasing LPS concentrations ranging from 10 to 100 ng/mL for 24 h showing no toxicity (Fig. 1*A*). This treatment caused an increase in nitrite production that was dose-dependent (Fig. 1*B*). It is important to note that a 10 ng/mL LPS concentration did not produce a significant increase in nitrite production, the final product of iNOS activity. The different concentrations of G3 bisphosphonate (named G3bis) and G4 bisphosphonate (named G4bis) phosphorus dendrimers alone or in the presence of LPS (100 ng/mL) caused no toxicity in macrophages as determined by the percentage of lactate dehydrogenase (LDH) released to the culture medium. We also tested the toxicity of both neutral and cationic G4 PAMAM dendrimers alone or in the presence of LPS and found that while the cationic G4 PAMAM dendrimer showed toxicity, the neutral G4 PAMAM dendrimers did not. These data indicate that phosphorus dendrimers are not toxic to macrophages (Fig. S1).

Effect of G3bis and G4bis on LPS-Stimulated Mouse Peritoneal Macrophages. Initially, we characterized the inflammatory response of mouse peritoneal macrophages after treatment with LPS (100 ng/mL) by determining the secretion of different proinflammatory mediators such as the cytokines TNFα and IL-1β, the levels of surface receptor CD86, inducible nitric oxide synthase (iNOS) protein expression, and nitrite production. As it was expected, LPS induced an increase in all of the proinflammatory mediators studied, indicating a polarization of mouse peritoneal macrophages toward M1 population. LPS-treated mouse macrophages displayed an enhancement of iNOS expression that was time-dependent and reached maximal levels at 24 h (Fig. S2*A*), coinciding with the peak of nitrite production (Fig. S2*B*). Neutral phosphorus dendrimers G3bis and G4bis did not have any effect on nitrite production by themselves (Fig. S3), but they strongly prevented the increase in nitrite production in a concentration-dependent manner, G4bis being more potent than G3bis (IC_{50} of 0.88 μM and 2.20 μM, respectively) (Fig. 2*A*). The reduction of NO levels might be related to inhibition of iNOS expression since both G3bis and G4bis reduced LPS-induced iNOS expression in a concentration-dependent manner (Fig. 2 *B* and *C*).

Moreover, LPS induced the release of the proinflammatory cytokines TNF-α and IL-1β in mouse peritoneal macrophages. TNF-α reached maximal levels 6 h after stimulation, whereas IL-1β showed maximal levels at 24 h (Fig. 3*A*). Interestingly, G3bis and G4bis reduced LPS-induced TNF-α and IL-1β secretion in a concentration-dependent manner, the effect on IL-1β levels being more potent (Fig. 3 *B* and *C*).

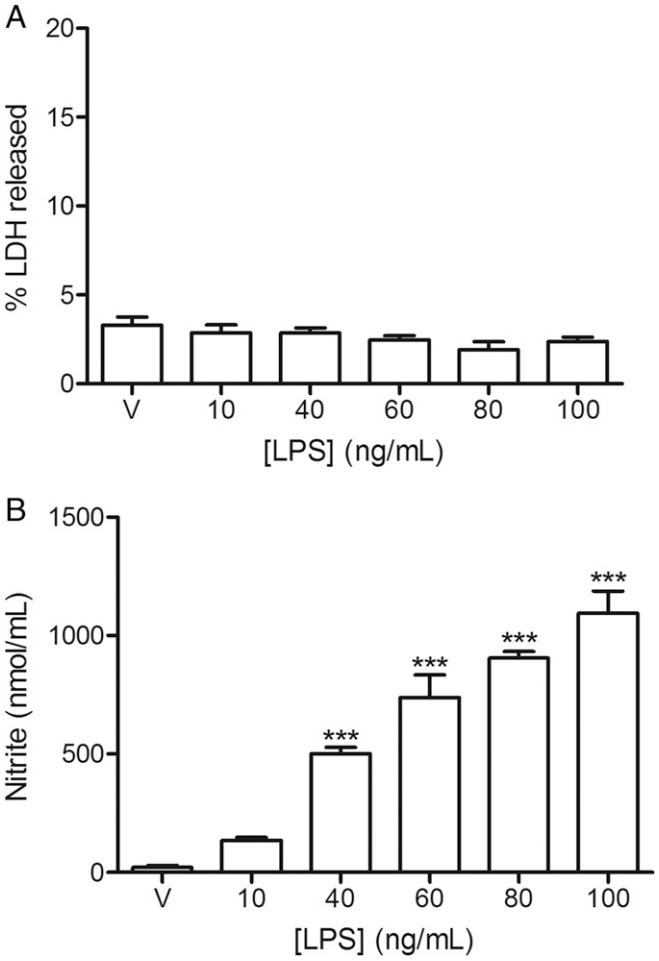

Fig. 1. Effect of LPS on mouse peritoneal macrophages viability and nitrite production. Mice macrophages were exposed to increasing LPS concentrations for 24 h and (*A*) LDH release to the culture medium or (*B*) nitrite production were determined as indicated in *Methods*. V represents cells treated with culture medium containing $1^0/_{00}$ DMSO. Data are expressed as mean ± SEM from 6 to12 determinations from at least three different cell cultures. ***$P < 0.001$, compared with vehicle-treated cells.

In addition, LPS treatment also increased the levels of CD86 expression at 24 h supporting the role of LPS in inducing macrophages polarization toward M1 classical pattern of activation (Fig. 4). Both G3bis and G4bis reduced LPS-induced CD86 expression significantly (Fig. 4), suggesting that these nanoparticles inhibited macrophage M1 polarization.

One possible explanation for this marked inhibitory effect of these neutral phosphodendrimers might be that the dendrimers are simply binding LPS, preventing the proinflammatory activity on macrophages. To exclude this possibility, and since it is not possible to change completely the medium to remove the dendrimer because this procedure activates macrophages, making it impossible to determine the basal level of macrophage inflammatory status, peritoneal macrophages were treated for 1 h with either vehicle or LPS 100 ng/mL, and then culture medium alone or containing G3bis or G4bis phosphodendrimers (final concentration 1 or 10 μM) were added to dilute LPS to a final concentration of 10 ng/mL that, as shown in Fig. 1, does not cause a significant increase in nitrite production. Macrophages were then incubated for additional 23 h. Afterward, supernatants were collected to quantify nitrite, and cell lysates were obtained to study iNOS expression. As it can be observed in Fig. 5, beside being added 1 h after LPS, both G3bis or G4bis phosphodendrimers were

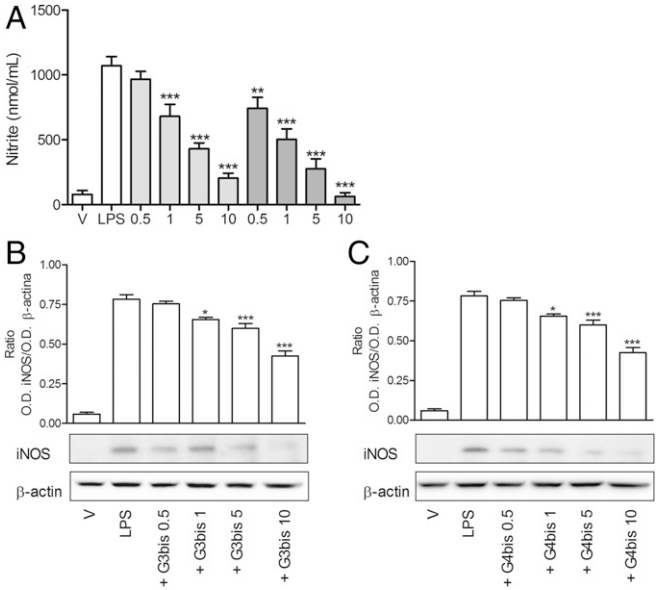

Fig. 2. Effect of increasing concentrations of G3bis- and G4bis-phosphorus dendrimers (in micromolar) on LPS (100 ng/mL)-induced nitrite production and iNOS expression. (*A*) Nitrite release from mouse macrophages following LPS treatment for 24 h was markedly inhibited in a concentration-dependent manner by the presence of G3bis- (light gray) and G4bis (dark gray) -phosphorus dendrimers. V represents cells treated with culture medium containing $1^0/_{00}$ DMSO. Data are expressed as mean ± SEM of 6 to12 determinations from at least three different cell cultures. $^{**}P < 0.01$; $^{***}P < 0.001$, compared with LPS-treated cells. Western blot image showing the effect of increasing doses of (*B*) G3bis- and (*C*) G4bis-phosphodendrimers on LPS (100 ng/mL)-induced iNOS expression. The image shows one experiment that was repeated three times with similar results and the ratio between the optical densities of iNOS and β-actin after densitometric analysis of the Western blot experiments. Graph data represent mean ± SEM from three experiments. $^{*}P < 0.05$; $^{**}P < 0.01$; $^{***}P < 0.001$, compared with LPS-treated cells.

able to decrease nitrite formation, suggesting that the antiinflammatory effect was not due to a physical interaction between LPS and the phosphodendrimers. Moreover, a G4 neutral PAMAM dendrimer (10 μM) did not show any significant effect on LPS-mediated nitrite production or iNOS induction when added to macrophages 1 h after LPS, suggesting that the antiinflammatory effect was specific for phosphodendrimers (Fig. 5).

Since NFkB activation has been described to play a central role in the induction of most of the proinflammatory mediators studied in this work, we determined the effect of phosphorus dendrimers on LPS-induced NFkB activation. First, we studied the time course of LPS-induced NFkB activation and observed that LPS induced a rapid translocation of the transcription factor from cytosol to nucleus, reaching maximal levels in nuclear fraction at 60 min as previously described (17) (Fig. 6*A*). Thus, this time point was selected to perform the following experiments. Both G3bis and G4bis phosphorus dendrimers markedly inhibited NFkB activation by preventing NFkB translocation from cytosol to nucleus, allowing NFkB accumulation in the cytosol. MG132, a proteasome inhibitor, was used as positive control. As it can be observed in Fig. 6*B*, G3bis and G4bis prevented NFkB activation to a similar extent as the reference compound MG-132.

Taking together, the data suggested that these phosphorus dendrimers were able to inhibit LPS-induced macrophage activation, displaying an interesting antiinflammatory profile.

G3bis and G4bis Prevent LPS-Mediated M1 Polarization of Mouse Macrophages. To determine whether the antiinflammatory effect of the phosphorus dendrimers was due to the induction of macrophage polarization toward the M2 alternative pattern of activation, we studied the levels of IL-4 and CD163 expression as

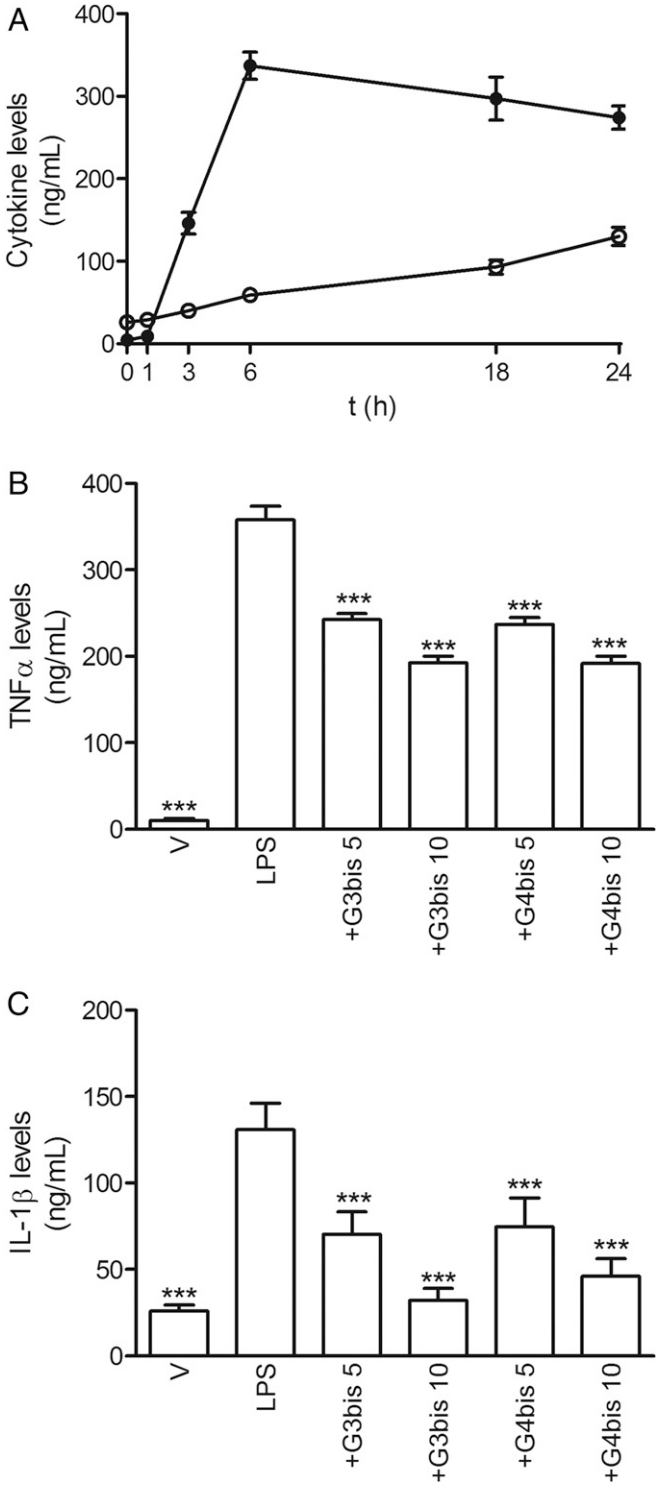

Fig. 3. Effect of phosphorus dendrimers on LPS-induced proinflammatory cytokine secretion by mouse macrophages. (*A*) Time course of LPS (100 ng/mL)-induced secretion of TNFα (●) and IL-1β (○) from mouse macrophages. (*B*) G3bis- and G4bis-phosphorus dendrimers (in micromolar) reduced LPS (100 ng/mL)-induced TNFα at 6 h; and (*C*) IL-1β (at 24 h) production in a concentration-dependent manner. V represents cells treated with culture medium containing $1^0/_{00}$ DMSO. Data represent mean ± SEM of 6 to 12 determinations from at least three different cell cultures. $^{***}P < 0.001$ compared with LPS-treated cells.

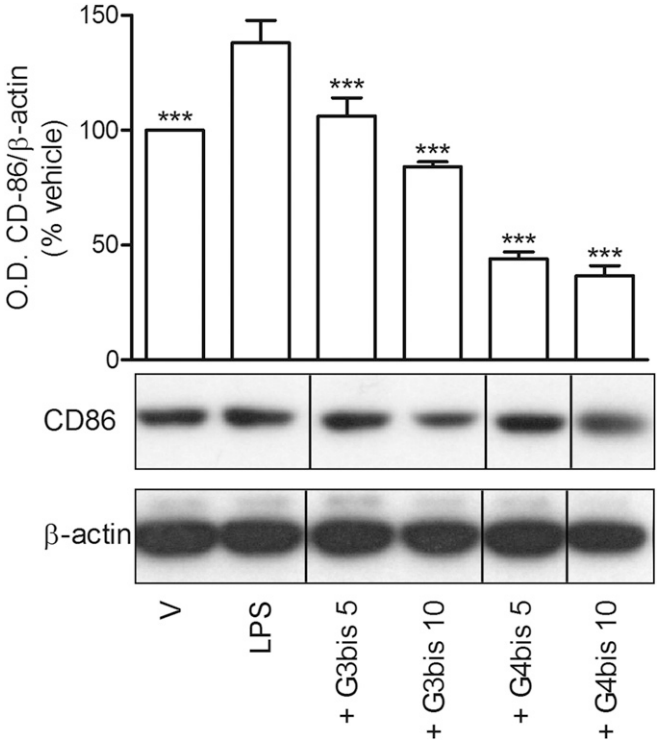

Fig. 4. Effect of phosphorus dendrimers on LPS (100 ng/mL)-induced CD86 expression after treatment for 24 h. Western blot image showing the effect of increasing concentrations (in micromolar) of G3bis- and G4bis-phosphorus dendrimers on LPS (100 ng/mL)-induced CD86 expression in mouse macrophages. V represents cells treated with culture medium containing $1^0/_{00}$ DMSO. The image shows one experiment that was repeated three times with similar results. The graph represents the ratio between the optical densities of CD86 and β-actin after densitometric analysis of the Western blot experiments. Data are expressed as mean ± SEM from three experiments. Black vertical lines between gel bands indicate gel band splicing. $*P < 0.05$; $***P < 0.001$ compared with LPS-treated cells.

markers for M2 population. While LPS significantly reduced the levels of IL-4 after 24 h (Fig. 7*A*), G3bis and G4bis prevented this effect (Fig. 7*B*). Moreover, CD163 was reduced in response to LPS exposure (Fig. 7*C*), while both G3bis and G4bis restored CD163 levels in a concentration-dependent manner. G4bis restored CD163 basal levels at the highest concentration assayed (Fig. 7*C*).

These results suggest that G3bis and G4bis neutral phosphorous dendrimers prevent macrophages from polarizing to M1 state and return the balance M1/M2 toward a noninflammatory situation.

Antiinflammatory Properties of the Phosphorus Dendrimers in Vivo. To determine whether these nanoparticles also displayed an antiinflammatory profile in vivo, we studied the effect of both G3bis and G4bis on an in vivo model of subchronic inflammation, the mouse air pouch injected with zymosan. To this end, zymosan was injected into the generated air pouch to induce an inflammatory response and G3bis or G4bis dendrimers were injected either in the air pouch (Fig. S4) as generally done to test antiinflammatory effects of different compounds or i.v. (Fig. 8) to prevent a possible direct interaction between zymosan and the phosphorus dendrimers that might explain the effect without the need for an antiinflammatory action. The effect of the dendrimers on cell infiltration, nitrite levels, and iNOS expression in the infiltrated cells was determined. In addition, the tissues surrounding the air pouch were collected and the expression of CD86 and CD163 was also analyzed.

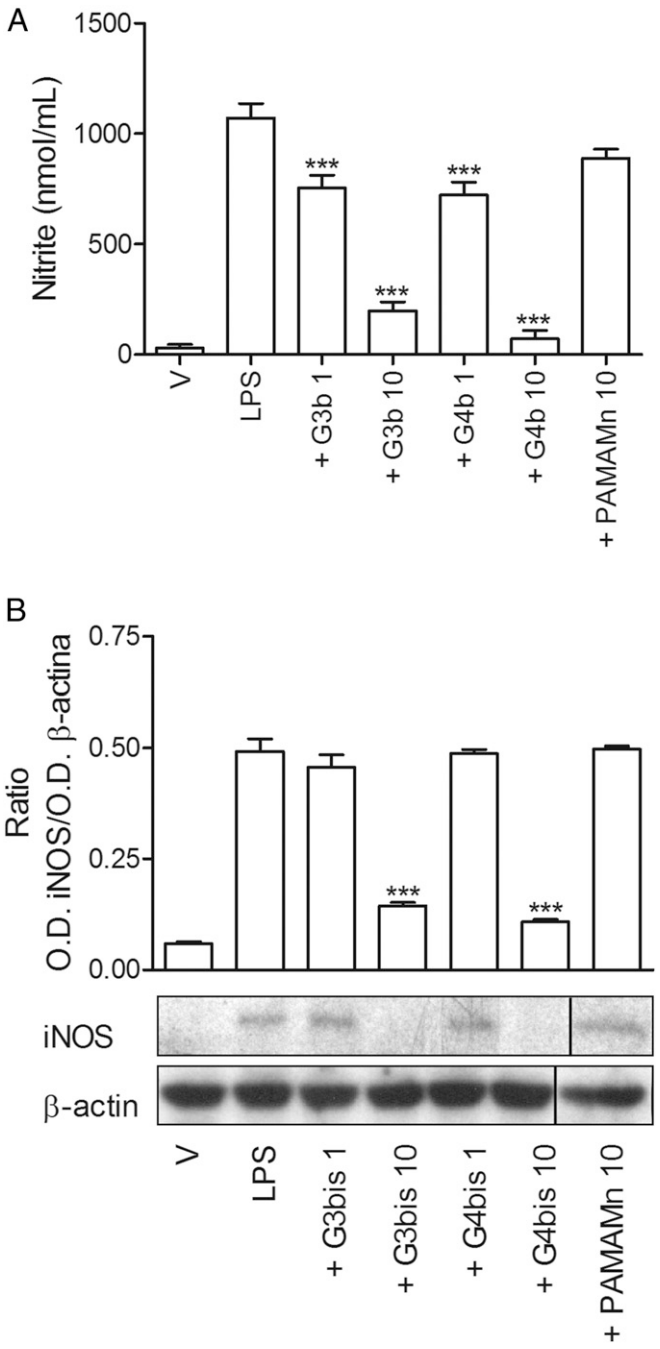

Fig. 5. Effect of delayed addition of G3bis and G4bis on LPS (100 ng/mL)-induced nitrite production and iNOS expression. Mouse peritoneal macrophages were treated with LPS (100 ng/mL) for 1 h and then diluted to 10 ng/mL using a solution that contained either culture medium or the indicated phosphorus dendrimer, to achieve a final concentration of 1 or 10 μM, or neutral G4 PAMAM dendrimer to achieve 10 μM. Cells were incubated for additional 23 h and (*A*) nitrite release or (*B*) iNOS induction were determined. V represents cells treated with culture medium containing $1^0/_{00}$ DMSO. Data are expressed as mean ± SEM of 6 to12 determinations from at least three different cell cultures for nitrite release while the Western blot image shows one experiment that was repeated three times with similar results and the ratio between the optical densities of iNOS and β-actin after densitometric analysis of the Western blot experiments. Black vertical line between gel bands indicates gel band splicing. $***P < 0.001$, compared with LPS-treated cells.

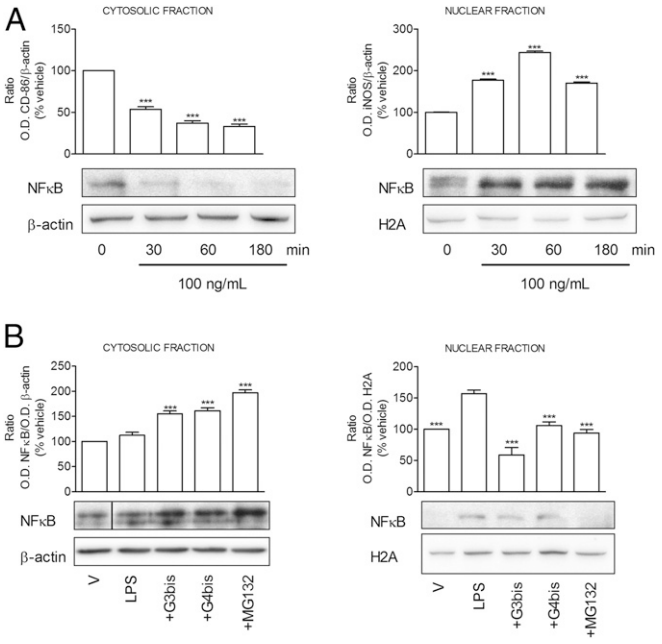

Fig. 6. Effect of phosphorus dendrimers on LPS (100 ng/mL)-induced NFkB translocation from cytosol to nucleus. (*A*) Time course of LPS (100 ng/L)-induced NFkB levels in cytosolic and nuclear fractions. Western blot images show one experiment that was repeated three times with similar results. The graph represents the ratio between the optical densities of NFkB and β-actin for cytosolic fraction and NFkB and histone H2A for nuclear fraction after densitometric analysis of the Western blot experiments. Data are expressed as mean ± SEM from three experiments. ***$P < 0.001$ compared with time 0. (*B*) Effect of G3bis- and G4bis-phosphorus dendrimers (10 μM) on LPS (100 ng/mL)-induced NFkB levels in cytosolic and nuclear fractions. MG-132 (1 μM) is a proteasome inhibitor used as control. V represents cells treated with culture medium containing $1^0/_{00}$ DMSO. Western blot images shows one experiment that was repeated three times with similar results. The graph represents the ratio between the optical densities of NFkB and β-actin for cytosolic fraction and NFkB and histone H2A for nuclear fraction after densitometric analysis of the Western blot experiments. Data are expressed as mean ± SEM from three experiments. Black vertical line between gel bands indicates gel band splicing. Background for H2A gel in *B* was homogeneously reduced. ***$P < 0.001$ compared with LPS-treated cells.

As shown in Fig. 8, G3bis and G4bis significantly reduced the number of migrated cells into the pouch and also the pouch nitrites levels (Fig. 8 *A* and *B*), G4bis being slightly more potent than G3bis. Reduction of nitrite levels was accompanied by a reduction of iNOS expression in the cells migrated into the pouch (Fig. 8*C*). Western blot studies showed that G3bis and G4bis significantly reduced iNOS expression in infiltrated cells and cells lining the air pouch cavity and reduced CD86 expression, whereas restored CD163 expression in cells lining the air pouch cavity (Fig. 8*D*). Taking together, our data suggest that these high-generation neutral phosphorus dendrimers display an interesting antiinflammatory profile and are able to modulate the M1/M2 ratio in vivo as well as in vitro. These results were very similar to those obtained by intrapouch administration of G3bis and G4bis phosphodendrimers (Fig. S4).

To further exclude a physical interaction between the phosphodendrimers and zymosan, dynamic light-scattering experiments were performed on a solution of either G4bis dendrimer (the largest dendrimer used in the study) because this dendrimer possibly might have the greater interaction/steric effect with zymosan and on solutions containing different concentrations of both dendrimer and zymosan (range from 0.1 to 0.8 mg/mL) as well as on those containing the same concentration of the two components (0.25 mg/mL) to avoid a possible effect due to a too-large excess of dendrimer. It was found that the size of the dendrimer alone ranged between 5 and 5.5 nm and that the size of the dendrimer in the presence of zymosan was between 5.4 and 5.8 nm (Fig. S5). Taking into account that the size of zymosan itself is about 3 μm, these experiments suggest the probable absence of interactions between the dendrimer and zymosan. No change was observed in the size of zymosan, which presents the same polydispersity before and after addition of the dendrimer. Moreover, neither ^{31}P NMR or ^{1}H NMR showed any kind of interaction between G4bis and zymosan (Figs. S6 and S7). Diffusion-ordered spectroscopy (DOSY) ^{1}H NMR experiments indicated that the self-diffusion coefficient (noted D), measured for dendrimer in the presence of zymosan ($D = 3.2 \times 10^{-10}$ m^2 s^{-1}) was significantly smaller than that determined for the dendrimer alone ($D = 6.3 \times 10^{-11}$ m^2 s^{-1}) (Fig. S8). Such observation indicates a fast exchange (on the NMR timescale) between free dendrimer and dendrimer in interaction with the slowly diffusing zymosan ($D = 0.6 \times 10^{-11}$ m^2 s^{-1}). The observed diffusion coefficients are the weighted average of the zymosan-linked and free dendrimers in solution; the observed diffusion coefficient D_{av} is then equal to $D_{av} = x_{int} \times D_{zymosan} + (1 - x_{int}) \times D_{dendfree}$, where x and D correspond to the molecular fraction and the diffusion coefficient of the free dendrimer and of the dendrimer bound to zymosan, respectively. Such values indicate that a part of the free dendrimer (55%) is in fast exchange with zymosan, suggesting a weak interaction (Fig. S8).

G3bis and G4bis also Exert Antiinflammatory Properties on Human Macrophages. Since the phosphorus dendrimers studied shown an interesting antiinflammatory profile in mice both in vitro and in vivo by modulating M1/M2 polarization, next we explored the effect of these nanoparticles on human monocyte-derived macrophages.

To this end, peripheral blood mononuclear cells (PBMCs) were isolated on a Ficoll-Hypaque density gradient (Rafer) from buffy coats obtained from the transfusion center, as indicated in *Methods,* and following national guidelines were grown in the presence of GM-CSF to obtain monocyte-differentiated M0 macrophages. Afterward, human macrophages were stimulated with LPS (100 ng/mL) in the absence or presence of G3bis and G4bis, and NFkB, iNOS and CD86 expression, nitrite levels, and toxicity were evaluated. G3bis and G4bis alone or in the presence of LPS did not modify the viability of monocyte-differentiated macrophages. LPS treatment induced an increase in CD86, iNOS expression, and NFkB activation that was significantly prevented by both G3bis and G4bis with a similar potency to that displayed in mice (Fig. 9 *A–D*). In addition, G3bis and G4bis inhibited nitrite production in a concentration-dependent manner with a similar intensity to that obtained in mouse macrophages (Fig. 9*E*). Taken together, these results strongly support the idea that these phosphorus dendrimers also have a promising antiinflammatory profile in human macrophages by preventing polarization to an M1 state and return the balance M1/M2 toward a noninflammatory situation.

Discussion

Macrophages can play a dual role in many inflammatory diseases depending on the phenotype that is induced. So, activation leading to the proinflammatory M1 phenotype induces the release of proinflammatory mediators such as reactive oxygen species, cytokines, and NO that might contribute to the tissue lesion caused by the inflammatory response as in, for instance, multiple sclerosis (4). In addition, activation of the M1 phenotype leads to the expression of biomarkers such as CD40, CD86, CD64, and CD32. However, macrophage polarization toward M2 phenotype reduces inflammation, and in the case of multiple sclerosis, also promotes CNS repair by clearance of myelin debris and production of growth factors (18), therefore preventing the shifting of

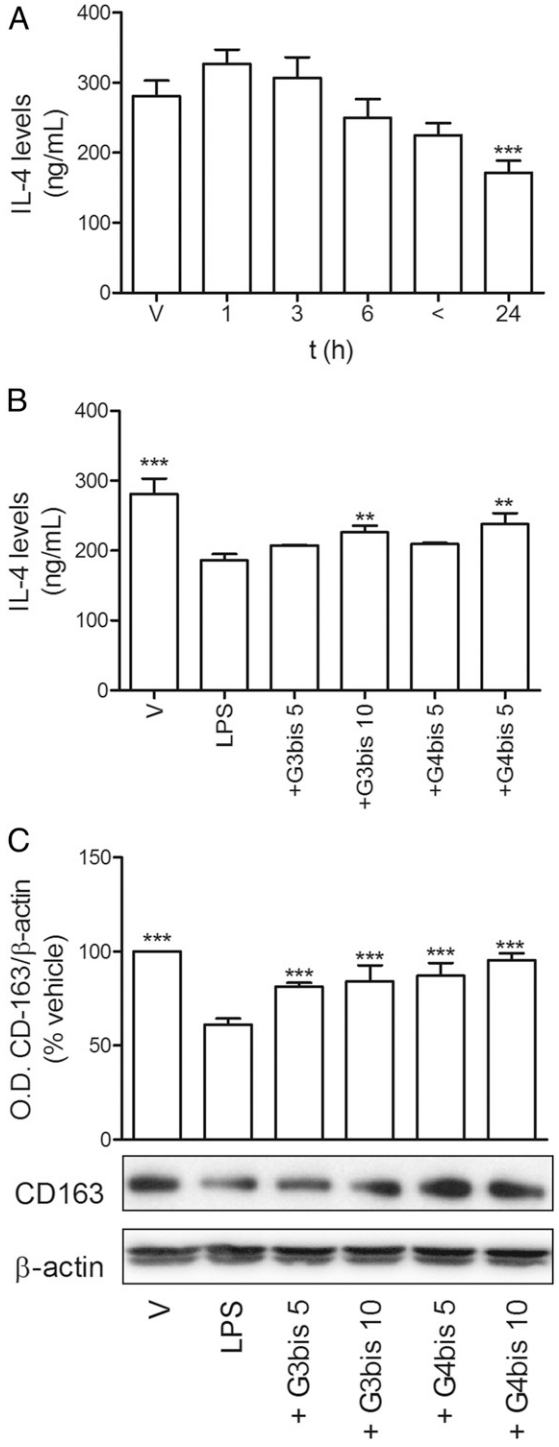

Fig. 7. Phosphorus dendrimers prevent LPS-induced M1 polarization of mouse macrophages. (*A*). LPS (100 ng/mL) reduced IL-4 production in mouse macrophages in a time-dependent manner. V represents time 0. ***$P < 0.001$ compared with V; (*B*) G3bis- and G4bis-phosphorus dendrimers (in micromolar) reversed LPS (100 ng/mL)-induced IL-4 reduction at the highest concentration studied (10 μM) at 24 h. V represents cells treated with culture medium containing $1^0/_{00}$ DMSO. **$P < 0.01$; ***$P < 0.001$ compared with LPS-treated cells. (*C*) G3bis- and G4bis-phosphorus dendrimers (in micromolar) prevented LPS (100 ng/mL)-induced decrease in CD163 expression 24 h after treatment. Western blot image shows one experiment that was repeated three times with similar results. The graph represents the ratio between the optical densities of CD163 and β-actin after densitometric analysis of the Western blot experiments. Data are expressed as mean ± SEM from three experiments. ***$P < 0.001$ compared with LPS-treated cells.

M1/M2 ratio of macrophage populations toward M1 state. This may be beneficial in treating some inflammatory diseases.

In agreement with data previously described, we have polarized a population of mouse macrophages to M1 classical pattern after treatment to LPS (7). These M1 macrophages were characterized by increased TNFα, IL-1β and nitrite production, NFkB activation, and iNOS and CD86 expression, all of them markers for M1 population (2, 7). Interestingly, both phosphorus dendrimers G3bis and G4bis strongly prevented macrophage M1 polarization by blocking NFkB activation. The NFkB family of proteins is formed by heterodimers and homodimers that are sequestered in the cytosol by members of the IkB family. In response to several stimuli, including LPS, IkB kinase is activated and phosphorylates IkB on serine residues result in dissociation of the NFkB/IkB complex. Free NFkB dimers can then translocate to the nucleus, bind to enhancer target genes, and increase the expression of different proinflammatory proteins such as TNFα, IL-1β, iNOS, and CD86 (5). In agreement with this, we observed that prevention of NFkB activation correlated with reduced levels of TNFα, IL-1β, and nitrite, as well as with reduced iNOS and CD86 expression. Therefore, the results obtained indicated that both G3bis and G4bis neutral phosphorus dendrimers were able to prevent macrophage polarization to M1 classical activation pattern in response to a well-known inducer of M1 activation such as LPS. One possible explanation for these results might be that there is a direct interaction between LPS and phosphodendrimers that precludes LPS action. However, when phosphodendrimers were added 1 h after LPS (100 ng/mL), causing a dilution of LPS to 10 ng/mL, a concentration that was not able to induce iNOS expression or nitrite production during 24 h (Fig. 1), they maintained their inhibition on LPS-induced inflammatory actions, suggesting that a direct LPS/phosphodendrimer interaction does not play a role in this antiinflammatory phosphodendrimer action. Moreover, 1 h after LPS addition, it is likely that LPS induction of intracellular signaling leading to the inflammatory response has already taken place, which would suggest that the phosphodendrimer antiinflammatory action takes place intracellularly.

On the other hand, M2 macrophages release a variety of antiinflammatory cytokines such as IL-4 (2). LPS reduces IL-4 levels as it polarizes macrophages toward M1 population (19). Both G3bis and G4bis dendrimers restored the levels of IL-4 reduced after LPS treatment, suggesting that both G3bis and G4bis restored the basal M1/M2 polarization ratio. It is well-known that the switching to the antiinflammatory M2 population is correlated with an increase in CD163 expression (20). CD163 is one of the members of the scavenger receptor cysteine-rich superfamily selectively expressed in M2 macrophages (21) and CD163 positive macrophages are frequently found during the healing phase of acute inflammation. Conversely, proinflammatory stimuli such as LPS or TNFα reduce CD163 protein expression (21). Both G3bis and G4bis restored CD163 levels reduced by LPS treatment, and even increased CD163 expression at the higher concentration assayed, supporting the hypothesis that G3bis and G4bis could modify M1/M2 ratio toward the basal ratio.

In view of the interesting profile showed by G3bis and G4bis on LPS-challenged mouse macrophages, we explored whether this antiinflammatory profile was also present in an in vivo model of subchronic inflammation. The air pouch model for induction of inflammation, first introduced by Selye in 1953 (22), has the advantage of supplying a suitable space for the induction of inflammatory responses and for studying the antiinflammatory properties of different compounds in vivo. It is well-established that zymosan injection into the air pouch causes a marked but slower leukocyte influx into the pouch formed mainly by polymorphonuclear leukocytes (PMNs) but also by monocytes. In addition, the air pouch cavity is mainly composed of macrophages that may regulate the inflammatory response into the

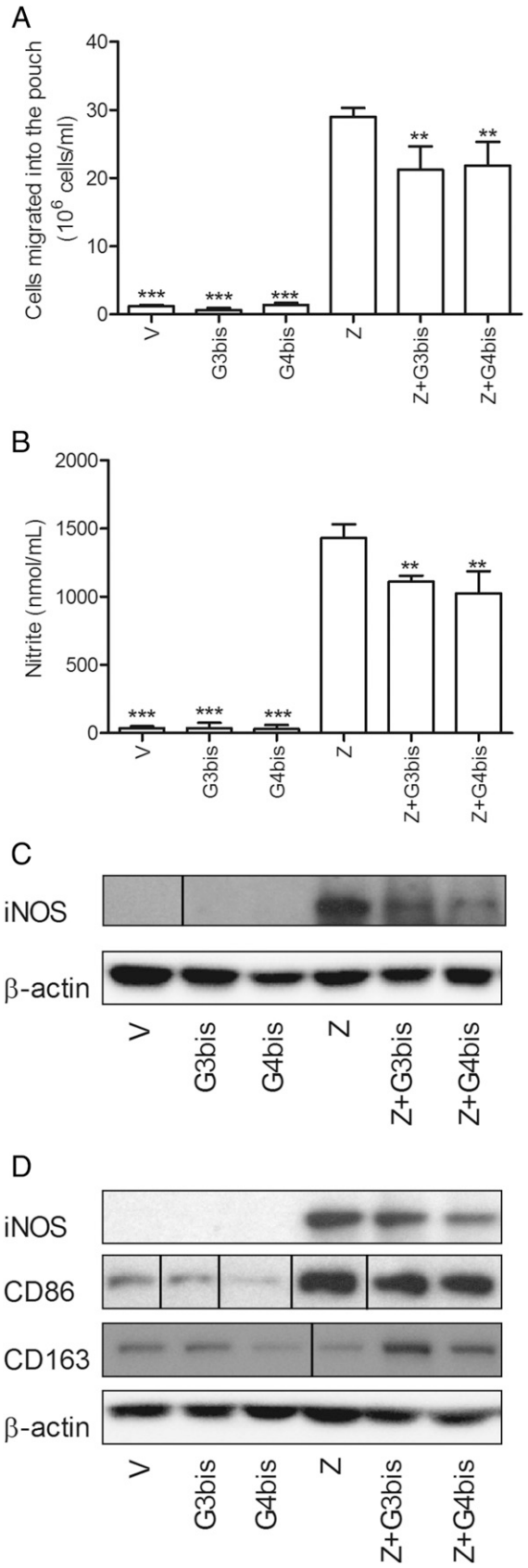

Fig. 8. Phosphorus dendrimers show antiinflammatory actions in the zymosan-injected air pouch model of subchronic inflammation. i.v.-injected G3bis- and G4bis-phosphorus dendrimers (10 mg/kg) (*A*) reduced cell infiltration into the mouse air pouch, (*B*) diminished nitrite production, (*C*) inhibited iNOS expression in the cells migrated into the pouch in response to zymosan, and (*D*) reduced zymosan-induced iNOS and CD86 expression in the cells surrounding the cavity while preventing zymosan-mediated decrease in CD163. V represents cells treated with culture medium containing $1^0/_{00}$ DMSO. Western blot images show one experiment that was repeated three times with similar results. Data represent mean ± SEM from four animals. Black vertical lines between gel bands indicate gel band splicing. $^{**}P < 0.01$; $^{***}P < 0.001$ compared with zymosan-treated group.

pouch (17, 23). i.v. G3bis and G4bis reduced cell infiltration into the air pouch and significantly reduced nitrite production. The reduction of nitrite levels could be directly related to the reduction of cells migrated into the pouch, but also to an inhibition of iNOS expression. In this regard, we have observed that both dendrimers significantly reduced iNOS expression in the cells that migrated into the pouch and also in cells lining the air pouch. Therefore, although the contribution of inhibition of leukocyte migration could not be discarded, the data strongly point to that the reduction in nitrite levels is mainly related to reduced iNOS expression. Interestingly, considering that leukocytes infiltrated into the air pouch are mainly PMNs (17), our data might suggest a possible modulation of the inflammatory response of PMNs. Moreover, we have also studied the inflammatory pattern of the macrophages lining the air pouch and have observed that G3bis and G4bis reduced CD86 expression and increased CD163 expression, suggesting that both nanoparticles induced M2 polarization of macrophages lining the cavity, contributing to the antiinflammatory effect observed. To completely exclude that a direct interaction between zymosan and phosphorus dendrimers might contribute to the in vivo antiinflammatory effects observed when, in an additional experiment, phosphorus dendrimers were directly injected in the air pouch (Fig. S4), DOSY experiments were performed and showed a fast exchange between G4bis and zymosan, suggesting that at high zymosan (5 mg in 1 mL DMSO) concentration, some weak interactions can be found as exemplified by a significant difference of the diffusion coefficient when moving from the dendrimer to the mixture dendrimer/zymosan. However, at the concentrations used in the experiments reported in the article no interaction can be clearly observed, excluding a direct interaction between phosphodendrimers and zymosan (Fig. S8). Moreover, the phosphorous and proton NMR experiments as well as dynamic light-scattering (DLS) experiments did not show a direct phosphodendrimer/zymosan interaction. Indeed, the most probable interaction which might be expected should be between the OH groups of zymosan and the P(O) (OMe) 2 terminal groups of the dendrimer mainly due to the hydrophobic character of the interior of the dendrimer. In this case we should observe a shift of the signal of the P(O) (OMe)2 in the ^{31}P NMR that was not the case (Fig. S6). Moreover, no clear differences are detected in ^{1}H NMR, but only a very slight shift (a few hertz) is observed at 3.3 ppm for the terminal OMe groups of the dendrimer whatever the dendrimer/zymosan ratio (Fig. S7). In addition, the in vivo antiinflammatory effect of both G3bis and G4bis dendrimers achieved by i.v. injection also precludes that the observed antiinflammatory effect would be produced by complexation of zymosan by phosphodendrimers.

The antiinflammatory properties of G3bis and G4bis phosphorus dendrimers were also observed in human inflammatory cells, more precisely on monocyte-differentiated M0 macrophages polarized to an M1 state by LPS stimulation. Similarly to that observed in mouse tissue macrophages, G3bis and G4bis prevented LPS-induced NFkB activation and also significantly reduced NO production and iNOS and CD86 expression, suggesting that the antiinflammatory mechanism activated by G3bis and G4bis phosphorus dendrimers is also effective in human macrophages. This would support a possible therapeutic role of high-generation phosphorus dendrimers in inflammatory diseases.

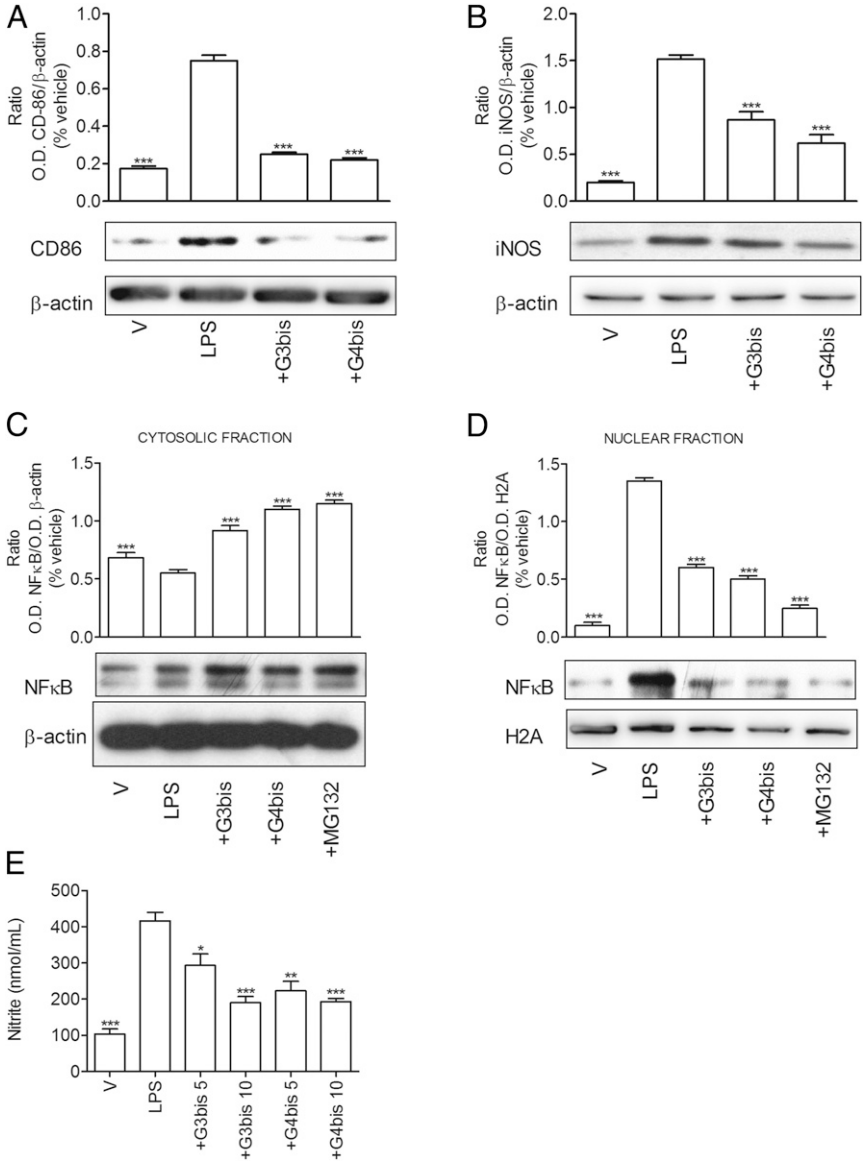

Fig. 9. Phosphorus dendrimers show antiinflammatory effects on LPS-stimulated monocytes-derived human macrophages. G3bis- and G4bis-phosphodendrimers (10 μM) inhibited LPS (100 ng/mL)-mediated increase in (*A*) CD86 and (*B*) iNOS expression; NFkB translocation from (*C*) cytosol to (*D*) the nucleus and (*E*) LPS (100 ng/mL)-mediated increase in nitrite production in monocytes-derived human macrophages. V represents cells treated with culture medium containing $1^0/_{00}$ DMSO. Western blot images show one experiment that was repeated three times with similar results. Graphs represent the ratio between optical densities of the indicated proteins after densitometric analysis of the Western blot experiments. Data are expressed as mean ± SEM from three experiments (*A*–*D*) and from 6 to12 determinations from at least three different cell cultures (*E*). Background for β-actin gel in *C* was homogeneously reduced. $*P < 0.05$; $**P < 0.01$; $***P < 0.001$, compared with LPS-treated cells.

Methods

Chemical Synthesis. Synthesis of dendrimer G3 bis and G4 bis bearing, respectively, 48 and 96 terminal bisphosphonate units: cesium carbonate ($n = 3$, 844 mg, 2.6 mmol; $n = 4$, 876 mg, 2.7 mmol) and phenol (500 mg, 1.31 mmol) were added to a solution of dendrimer G3 (290 mg, 0.027 mmol) or G4 (315 mg, 0.014 mmol) in THF (8 mL). The reaction mixture was stirred at room temperature for 1 d then centrifuged. The resulting clear solution was concentrated under reduced pressure (~3 mL) and then precipitated with a large excess of pentane. Unreacted phenol was removed by dissolving the resulting powder in 2–5 mL of THF and subsequent precipitation with an excess of pentane/ether to afford dendrimer G3 bis (Fig. 10), or G4 bis (Fig. 11) as a white powder (yield, respectively, 78 and 65%).

^{31}P-{^{1}H} NMR ($CDCl_3$, 121 MHz): δ = 7.61 (s, N_3P_3); 26.76 (s, PO_3Me_2); 62.60 (br s, P_1, and P_2); 63.02 (s, P_3); ^{1}H NMR ($CDCl_3$, 300 MHz): δ = 2.73 (t, $^3J_{HH}$ = 7.4 Hz, 96H, $\underline{CH_2}$-CH_2-N); 3.03 (t, $^3J_{HH}$ = 7.4 Hz, 96H, CH_2-$\underline{CH2}$-N); 3.15 (d, $^2J_{HP}$ = 9.5 Hz, 192H, *N*-CH_2-P); 3.39–3.25 (m, 126 H, $C_{0,1and\ 2}H_3$-*N*-P); 3.69 (d, $^3J_{HP}$ = 10.4 Hz, 576H, OMe); 7.08 (d, $^3J_{HH}$ = 8.2 Hz, 96H, CH arom); 7.16 (d, $^3J_{HH}$ = 8.2 Hz, 96H, CH arom); 7.22 (d, $^3J_{HH}$ = 8.2 Hz, 84H, CH arom); 7.62 (br s, 30H, C_1H = N and C_3H = N); 7.75–7.65 (m, 96H, CH arom and C_2H = N).**^{13}C-{^{1}H} $CDCl_3$,** 75.4 MHz) δ = 32.9 (s, $\underline{CH_2}$–CH_2-N); 33.0 (s, *N*-CH_3); 49.4 (dd, $^1J_{CP}$ = 157.5 Hz, $^3J_{CP}$ = 7.3 Hz, *N*-CH_2-P); 52.6 (m, P-O-CH_3); 58.0 (t, $^3J_{CP}$ = 7.5 Hz, CH_2-$\underline{CH_2}$-N);121.1 (s,),121.7 (br.s.); 128.2(br.s.); 129.9(s.); 132.4 (br.s.); 136.6(s.); 138.9 (br.s., CH = N); 148.8 (d, $^2J_{CP}$ = 7.3 Hz); 151.3(br.s). Chemical formula: $C_{1007}H_{1486}N_{135}O_{378}P_{141}S_{42}$; molecular weight: 27,245.35; elemental analysis: C, H, N; calc: C, 44.39; H, 5.50; N, 6.94; found: C, 44.11; H, 5.40; N, 6.78.

^{31}P-{^{1}H} NMR ($CDCl_3$, 121 MHz): δ = 26.76 (s, PO_3Me_2); 62.56 (br s, P_1, P_2, and P_3); 63.97 (s, P_4); ^{1}H NMR ($CDCl_3$, 300 MHz): δ = 2.73 (br s, 192H, $\underline{CH_2}$-CH_2-N); 3.03 (br s, 192H, CH_2-$\underline{CH_2}$-N); 3.15 (d, $^2J_{HP}$ = 9.5 Hz, 384H, *N*-CH_2P); 3.39–3.25 (m, 270 H, $C_{0,1,2\ and\ 3}H_3$-*N*-P); 3.69 (d, $^3J_{HP}$ = 10.4 Hz, 1152 H, OMe); 7.08 (d, $^3J_{HH}$ = 8.2 Hz, 192H, CH arom); 7.16 (d, $^3J_{HH}$ = 6.4 Hz, 192H, CH arom); 7.22 (d, $^3J_{HH}$ = 7.7 Hz, 180H, CH arom); 7.62 (br s, 54H, C_1H = N, and C_4H = N); 7.75–7.65 (m, 216H, CH arom, C_2H = N, and C_3H = N). -^{13}C-{^{1}H} $CDCl_3$ 75.4 MHz): δ = 32.9 (s, $\underline{CH_2}$–CH_2-N); 33.0 (br. s, *N*-CH_3); 55.0 (dd, $^1J_{CP}$ = 157.8 Hz, $^3J_{CP}$ = 7.4 Hz,

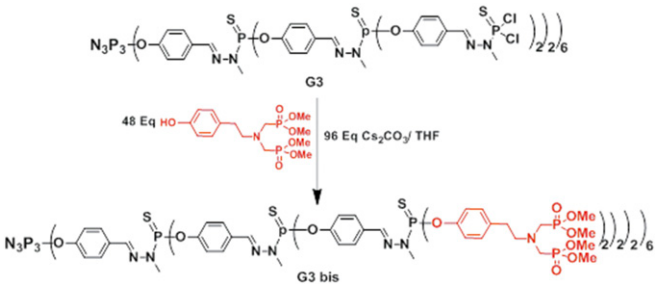

Fig. 10. G3bis neutral phosphorus dendrimer with 48 terminal bisphosphonate units.

N-CH_2-P); 52.6(m, P-O-CH_3); 58.0 (t, $^3J_{CP}$ = 7.5 Hz, CH_2- CH_2-N); 121.2 (s,),121.7 (br.s.); 128.2 (br.s.); 129.9 (s.); 132.3 (br.s.); 136.5 (s.); 138.6 (br.s., CH = N); 148.9 (d, $^2J_{CP}$ = 7.1 Hz); 151.3(br.s.).Chemical formula: $C_{2064}H_{3024}N_{279}O_{762}P_{267}S_{90}$; molecular weight: 55,058.13; elemental analysis: C, H, N; calc: C, 45.00; H, 5.53; N, 7.09; found: C, 44.89; H, 5.49; N, 6.99.

The purity of phosphorhydrazone dendrimers cannot be assessed by mass spectrometry (electrospray ionization or MALDI-TOF) as both techniques induce dramatic cleavages of the structure (24).

Animals. All animal care and experimental studies were conducted in accordance with the guidelines of the Ethical Committee of Animal Experimentation at University of Castilla-La Mancha. All studies involving animals are reported in accordance with guidelines of the European Union (2010/63/EU) for the use of laboratory animals and in accordance with the ARRIVE guidelines for reporting experiments involving animals (25, 26).

Cell Culture. Peritoneal macrophages were obtained as previously described (27). Female C57BL/6j mice (Janvier) weighing 25–30 g were used to obtain highly purified peritoneal macrophages. Cells were harvested by peritoneal lavage 4 d after i.p. injection of 1 mL 10% (wt/vol) thioglycollate broth and were resuspended in RPMI 1640 supplemented with 10% heat-inactivated FBS, 2 mM L-glutamine, 100 U/mL penicillin, and 100 μg/mL streptomycin. Cells were seeded at a concentration of 2×10^6 cells/mL in 24-well culture plate or 6-well culture plate for 2 h at 37 °C in a 5% CO_2 atmosphere incubator. The nonadherent cells were removed by two washes with culture medium. Adherent macrophages were used to perform the following experiments.

Human monocytes were isolated and purified from PBMCs of buffy coats (Servicio de Donantes, Hospital Universitario) using Ficoll-Hypaque (GE Healthcare) according to the manufacturer's instructions. The mononuclear cell interphase obtained by Ficoll-Paque density gradient centrifugation was obtained, and the cells were resuspended in RPMI 1640 supplemented with 10% heat-inactivated FBS, 2 mM L-glutamine, 100 U/mL penicillin, and 100 μg/mL streptomycin. Cells were seeded at a concentration of 2×10^6 cells per mL in 24-well culture plate or 6-well culture plate for 2 h at 37 °C in a 5% CO_2 atmosphere incubator. The nonadherent cells were removed by two washes with culture medium. Adherent monocytes were induced to differentiate for 7 d in the presence of recombinant human GM-CSF (25 ng/mL) to obtain M0 macrophages as previously described (28). Monocyte-differentiated M0 macrophages were used to perform the following experiments.

Characterization of Dendrimer/Zymosan Interaction. NMR spectra were recorded with Bruker AV 300 and AV 400 spectrometers. All spectra were measured at 25 °C in deuterated THF or DMSO. References for NMR were H_3PO_4 (85%) for ^{31}P NMR, $SiMe_4$ for ^1H and ^{13}C NMR spectroscopy.

DLS determinations of G4bis alone or in the presence of zymosan were performed using the Zetasizer Nano from Malvern. These experiments were conducted with 0.25 mg of G4bis in 1 mL DMSO and 0.25 mg of zymosan in 1 mL of DMSO but also by varying the amount of the two components (from 0.10 to 0.80 mg).

The 2D DOSY spectrum displays conventional chemical shift in one dimension and diffusion coefficient constants in the other dimension. Because of the relationship between diffusion coefficients and the molecular radii, the diffusion dimension reveals the distribution of molecular sizes and allows different molecular species to be unambiguously identified and assigned. This diffusion dimension is achieved by recording consecutive spectra in which the gradient strengths are incremented in a series of acquisitions. All diffusion measurements were made using the stimulated echo-pulse sequence with bipolar gradient pulses. The diffusion delay (Δ) was of 300 ms and the gradient pulse duration of 3.4 ms. The recycle delay was adjusted to 3 s. The diffusion dimension was processed with the Laplace inversion routine CONTIN (Topspin software). The observed diffusion coefficients are the weighted average of the zymosan-linked and free dendrimers in solution; the observed diffusion coefficient D_{av} is then equal to $D_{av} = x_{int} \times D_{zymosan} + (1 - x_{int}) \times D_{dendfree}$, where x and D correspond to the molecular fraction and the diffusion coefficient of the free dendrimer and of the dendrimer bound to zymosan, respectively.

Cell Viability. For viability experiments, LDH release was used as an index of cellular death as previously described (29). Briefly, cells were cultured in 24-well culture plates and treated with vehicle (dimethyl sulfoxide; 1‰ DMSO) or 100 ng/mL LPS in the presence or absence of different concentrations of phosphorus or PAMAM dendrimers (diluted in complete RPMI 1640 culture medium) for 24 h. Supernatants were then collected and cells were washed with PBS and lysed with 0.9% Triton X-100 (vol/vol) in saline. LDH activity released to culture media, as well as LDH present in lysates, was measured spectrophotometrically at 490 nm on a 96-well plate reader by using the Cytotox 96 Kit (Promega). Mortality was expressed as percentage of LDH released.

Quantification of Inflammatory Mediators. Cells cultured in 24-well culture plates were treated with vehicle (1‰ DMSO) or 100 ng/mL LPS in the presence or absence of different concentrations of phosphorus dendrimers for different times. Afterward, supernatants were collected and after centrifugation at 1,500 × *g* for 10 min at 4 °C, aliquots of the supernatants were used to measure different mediators. Nitrite production was quantified fluorometrically (30) in microtiter plates using a standard curve of sodium nitrite. The levels of the cytokines TNFα, IL-1β, and IL-4 were quantified by ELISA following manufacturer's instructions (Prepotech).

Extraction of Total Lysates. Cells were seeded in six-well culture plates and treated with vehicle (DMSO) or 100 ng/mL LPS in the presence or absence of different concentrations of phosphorus dendrimers for different times. Afterward, cells were washed twice with cold PBS and resuspended in homogenization buffer (10 mM Hepes, 0.32 M sucrose, 100 μM EDTA, 1 mM DTT, 0.1 mM PMSF, 40 μg/mL aprotinine, 20 μg/mL leupeptine; pH 7.4) (31). Cells were sonicated (two cycles, 10 s at maximum speed) at 4 °C in a VP 200S ultrasonic homogenizer at maximum potency (Hielscher Ultrasound Technology). Homogenates were centrifuged at 10,000 × *g* and supernatants, i.e., total lysates, were collected and stored at −80 °C until analysis by Western blotting.

Subcellular Fractionation: Isolation of Cytosolic and Nuclear Extracts. Nuclear and cytosolic extracts from macrophages were prepared as previously described (27). Cells seeded in six-well culture plates treated with vehicle (1‰ DMSO) or 100 ng/mL LPS in the presence or absence of different concentrations of phosphorus dendrimers or 5 μM MG-132 for different times. Afterward, cells were washed twice with ice-cold PBS, scraped, and collected by centrifugation at 1,500 × *g* for 10 min. Cell pellets were resuspended in extraction buffer A containing 10 mM Hepes, 1 mM EDTA, 1 mM EGTA, 10 mM KCl, 1 mM DTT, 5 mM FNa, 1 mM Na_3VO_4, 1 mg/mL leupeptin, 0.1 mg/mL aprotinin, 0.5 mM PMSF; pH 8. After 15 min on ice, Nonidet P-40 was added to reach a 0.5% concentration. Afterward, the samples were gently vortexed for 15 s, and nuclei were pelleted by centrifugation at 20,000 × *g* for 30 s at 4 °C. The supernatants, i.e., cytosolic extracts, were collected and stored at −80 °C until analyzed by Western blot. Pellets were resuspended in Buffer B containing 20 mM Hepes, 1 mM EDTA, 1 mM EGTA, 0.4 M NaCl, 1 mM DTT, 5 mM NaF, 1 mM Na_3VO_4, 1 mg/mL leupeptin, 0.1 mg/mL aprotinin, 0.5 mM PMSF; pH 8. Proteins were extracted by shaking samples for 30 min at 4 °C. Afterward, samples were centrifuged at 20,000 × *g* for 15 min. The supernatants, i.e., nuclear extracts, were collected and stored

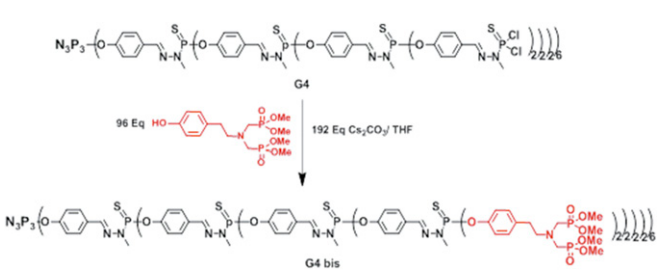

Fig. 11. G4bis neutral phosphorus dendrimer with 96 terminal bisphosphonate units.

at −80 °C until analysis by Western blot. No cross-contamination between these two fractions was observed.

Mouse Air Pouch Model. Air pouches were produced as previously described (27) by s.c. injection of 10-mL sterile air into the back of Female C57BL/6j mice (Janvier) weighing 25–30 g. Three days later 5-mL sterile air was injected into the same cavity. Six days after the initial air injection, animals were divided in six experimental groups (each one comprising four animals) that received the following treatments: (*i*) vehicle, sterile saline (1 mL) containing $1^0/_{00}$ DMSO in the air pouch; (*ii*) G3bis, 10 mg/kg i.v; (*iii*) G4bis, 10 mg/kg i.v; (*iv*) Zymosan, 1% wt/vol zymosan in saline in the air pouch; (*v*) Zymosan+G3 bis, 1% wt/vol zymosan in saline in the air pouch + G3bis, 10 mg/kg i.v; (*vi*) Zymosan+G4 bis, 1% wt/vol zymosan in saline in the air pouch + G4bis, 10 mg/kg i.v (Fig. 8).

In another set of experiments, all of the treatments were administered intrapouch, being the six experimental groups (each one comprising four animals) that received the following treatments injected (1 mL) in the air pouch: (*i*) vehicle, sterile saline containing $1^0/_{00}$ DMSO; (*ii*) G3bis, sterile saline + 10 μmol G3bis; (*iii*) G4bis, sterile saline + 10 μmol G4bis; (*iv*) Zymosan, 1% wt/vol zymosan in saline; (*v*) Zymosan+G3 bis, 1% wt/vol zymosan in saline + 10 μmol G3bis; (*vi*) Zymosan+G4 bis, 1% wt/vol zymosan in saline + 10 μmol G4bis. An additional dose of the appropriate phosphorus dendrimer (100 μL, 10 μM solution) was injected 8 h later into the air pouch of the phosphorus dendrimer-treated experimental groups. Vehicle and zymosan groups received a 100-μL saline injection (Fig. S4).

Twenty-four hours after beginning the experiment, mice were killed by cervical dislocation and the exudate in the pouch was collected by washing with 1 mL saline solution. The number of leukocytes present in the exudates were measured using a TC10 automated cell counter (Biorad). Exudates were centrifuged at 1,200 × *g* for 10 min at 4 °C and the supernatants used to measure nitrites. Cell pellets were resuspended in homogenization buffer (10 mM Hepes, 0.32 M sucrose, 100 μM EDTA, 1 mM DTT, 0.1 mM PMSF, 40 μg/mL aprotinine, 20 μg/mL leupeptine; pH 7.4) (31) and sonicated (two cycles, 10 s at maximum speed) at 4 °C in a VP 200S ultrasonic homogenizer at maximum potency (Hielscher Ultrasound Technology). The resulting homogenates were centrifuged at 1,200 × *g* for 10 min at 4 °C and supernatants stored at −80 °C until analysis by Western blot. The tissues surrounding the air pouch cavity were obtained and homogenized in buffer using an Omni TH homogenizer (Omni International). The resulting homogenates were centrifuged at 1,200 × *g* for 10 min at 4 °C and supernatants were stored at −80 °C until analysis by Western blot.

Western Blot Analysis. Immunoblot analysis was performed on total lysates, cytosolic and nuclear fractions, and homogenates obtained from the different experiments as previously described (32). Protein concentration was determined by using BCA protein assay kit and following manufacturer's instructions (Pierce Biotechnology). Protein samples (20 μg) were loaded on 12% PAGE-SDS and transferred onto nitrocellulose membranes. Membranes were blocked in PBS-Tween 20 (0.1%) containing 5% nonfat dry milk and 0.1% BSA for 1 h at 4 °C and then incubated with polyclonal anti-iNOS antibody (1:1,000), monoclonal anti-NFkB antibody (1:1,000), monoclonal anti-CD86 antibody (1:500), monoclonal anti-CD163 antibody (1:500), polyclonal β-actin antibody (1:2,000), or monoclonal anti-H2A antibody (1:1,000) overnight at 4 °C. Afterward, blots were washed with PBS-Tween 20 (0.1%) and incubated with HRP-anti-mouse IgG (1:10,000) or HRP-anti-rabbit IgG (1:10,000) for 2 h at 4 °C. Immunoreactive bands were visualized using an enhanced chemiluminescence system; Amersham Biosciences).

Drugs and Chemicals. BCA protein assay kit was obtained from Pierce Biotechnology Inc.; the Cytotox 96 kit from Promega Biotech Iberica S.L.; Ficoll-Hypaque from GE Healthcare ; and GM-CSF was from Immunotools. Cytokines kits were purchased from Preprotech. The following antibodies were used: iNOS (Cayman Chemical); NFkB (BD Transduction Laboratories); CD86 and CD163 (Abcam); anti-β-actin and anti-H2A antibodies (Cell Signaling) and HRP-conjugated IgG (DakoCytomation S.A.); PAMAM dendrimers were obtained from Nano-Synthons LLC. All other reagents were obtained from Sigma-Aldrich.

Statistical Analysis. Data are expressed as mean ± SEM. Statistical analyses were carried out using the one-way analysis of variance and the a posteriori Bonferroni's *t* test for multiple comparisons by using GraphPad software. *P* values less than 0.05 were considered significant (**P* < 0.05, ***P* < 0.01, ****P* < 0.001). Statistical significances are reported in the figure legends.

ACKNOWLEDGMENTS. We thank Vanesa Guijarro and Elena Galera for their expert technical assistance. This work was supported by the Spanish Ministerio de Economía y Competitividad (Grant BFU2014-59009-P) and Programa Iberoamericano de Ciencia y Tecnología para el Desarrollo (CYTED) (Grant 214RT0482) (to V.C.), and by CNRS (France).

1. Miron VE, et al. (2013) M2 microglia and macrophages drive oligodendrocyte differentiation during CNS remyelination. *Nat Neurosci* 16:1211–1218.
2. Jiang Z, Jiang JX, Zhang GX (2014) Macrophages: A double-edged sword in experimental autoimmune encephalomyelitis. *Immunol Lett* 160:17–22.
3. Mosser DM (2003) The many faces of macrophage activation. *J Leukoc Biol* 73: 209–212.
4. Vogel DY, et al. (2013) Macrophages in inflammatory multiple sclerosis lesions have an intermediate activation status. *J Neuroinflammation* 10:35.
5. Trinchieri G (2003) Interleukin-12 and the regulation of innate resistance and adaptive immunity. *Nat Rev Immunol* 3:133–146.
6. Nhu QM, Shirey KA, Pennini ME, Stiltz J, Vogel SN (2012) Proteinase-activated receptor 2 activation promotes an anti-inflammatory and alternatively activated phenotype in LPS-stimulated murine macrophages. *Innate Immun* 18:193–203.
7. Tannahill GM, Iraci N, Gaude E, Frezza C, Pluchino S (2015) Metabolic reprograming of mononuclear phagocytes in progressive multiple sclerosis. *Front Immunol* 6:106.
8. Posadas I, Monteagudo S, Ceña V (2016) Nanoparticles for brain-specific drug and genetic material delivery, imaging and diagnosis. *Nanomedicine (Lond)* 11:833–849.
9. Maszewska M, et al. (2003) Water-soluble polycationic dendrimers with a phosphoramidothioate backbone: Preliminary studies of cytotoxicity and oligonucleotide/plasmid delivery in human cell culture. *Oligonucleotides* 13:193–205.
10. Maksimenko AV, et al. (2003) Optimisation of dendrimer-mediated gene transfer by anionic oligomers. *J Gene Med* 5:61–71.
11. Solassol J, et al. (2004) Cationic phosphorus-containing dendrimers reduce prion replication both in cell culture and in mice infected with scrapie. *J Gen Virol* 85:1791–1799.
12. Mignani S, El Kazzouli S, Bousmina M, Majoral JP (2013) Expand classical drug administration ways by emerging routes using dendrimer drug delivery systems: A concise overview. *Adv Drug Deliv Rev* 65:1316–1330.
13. Blattes E, et al. (2013) Mannodendrimers prevent acute lung inflammation by inhibiting neutrophil recruitment. *Proc Natl Acad Sci USA* 110:8795–8800.
14. Degboé Y, et al. (2014) Modulation of pro-inflammatory activation of monocytes and dendritic cells by aza-bis-phosphonate dendrimer as an experimental therapeutic agent. *Arthritis Res Ther* 16:R98.
15. Caminade AM, Majoral JP (2016) Bifunctional phosphorus dendrimers and their properties. *Molecules* 21:538.
16. Hayder M, et al. (2011) A phosphorus-based dendrimer targets inflammation and osteoclastogenesis in experimental arthritis. *Sci Transl Med* 3:81ra35.
17. Posadas I, et al. (2000) Co-regulation between cyclo-oxygenase-2 and inducible nitric oxide synthase expression in the time-course of murine inflammation. *Naunyn Schmiedebergs Arch Pharmacol* 361:98–106.
18. Bogie JF, Stinissen P, Hendriks JJ (2014) Macrophage subsets and microglia in multiple sclerosis. *Acta Neuropathol* 128:191–213.
19. Sun LX, et al. (2017) The improvement of M1 polarization in macrophages by glycopeptide derived from *Ganoderma lucidum*. *Immunol Res* 65:658–665.
20. Gordon S (2003) Alternative activation of macrophages. *Nat Rev Immunol* 3:23–35.
21. Fabriek BO, Dijkstra CD, van den Berg TK (2005) The macrophage scavenger receptor CD163. *Immunobiology* 210:153–160.
22. Selye H (1953) Use of granuloma pouch technic in the study of antiphlogistic corticoids. *Proc Soc Exp Biol Med* 82:328–333.
23. Dawson J, Sedgwick AD, Edwards JC, Lees P (1991) A comparative study of the cellular, exudative and histological responses to carrageenan, dextran and zymosan in the mouse. *Int J Tissue React* 13:171–185.
24. Blais JC, Turrin CO, Caminade AM, Majoral JP (2000) MALDI TOF mass spectrometry for the characterization of phosphorus-containing dendrimers. Scope and limitations. *Anal Chem* 72:5097–5105.
25. Kilkenny C, Browne WJ, Cuthill IC, Emerson M, Altman DG (2010) Improving bioscience research reporting: The ARRIVE guidelines for reporting animal research. *J Pharmacol Pharmacother* 1:94–99.
26. McGrath JC, Drummond GB, McLachlan EM, Kilkenny C, Wainwright CL (2010) Guidelines for reporting experiments involving animals: The ARRIVE guidelines. *Br J Pharmacol* 160: 1573–1576.
27. Posadas I, De Rosa S, Terencio MC, Payá M, Alcaraz MJ (2003) Cacospongionolide B suppresses the expression of inflammatory enzymes and tumour necrosis factor-alpha by inhibiting nuclear factor-kappa B activation. *Br J Pharmacol* 138:1571–1579.
28. Montserrat-de la Paz S, et al. (2015) Pharmacological effects of mitraphylline from *Uncaria tomentosa* in primary human monocytes: Skew toward M2 macrophages. *J Ethnopharmacol* 170:128–135.
29. Monteagudo S, et al. (2012) Inhibition of p42 MAPK using a nonviral vector-delivered siRNA potentiates the anti-tumor effect of metformin in prostate cancer cells. *Nanomedicine (Lond)* 7:493–506.
30. Misko TP, Schilling RJ, Salvemini D, Moore WM, Currie MG (1993) A fluorometric assay for the measurement of nitrite in biological samples. *Anal Biochem* 214:11–16.
31. Knowles RG, Palacios M, Palmer RM, Moncada S (1990) Kinetic characteristics of nitric oxide synthase from rat brain. *Biochem J* 269:207–210.
32. Pérez-Carrión MD, et al. (2012) Dendrimer-mediated siRNA delivery knocks down Beclin 1 and potentiates NMDA-mediated toxicity in rat cortical neurons. *J Neurochem* 120:259–268.